processes

MDPI

Article

Research on Adsorption and Desorption Performance of Gas-Phase Naphthalene on Hydrophobic Modified FDU-15

Chunyu Zhao [1], Yingshu Liu [1,2], Miaomiao Meng [1], Ziyi Li [1,2], Haihong Wang [3], Wenhai Liu [1,2] and Xiong Yang [1,2,*]

[1] School of Energy and Environmental Engineering, University of Science and Technology Beijing, Beijing 100083, China; cyzhao@generalaire.cn (C.Z.); ysliu@ustb.edu.cn (Y.L.); tiffanymmm@163.com (M.M.); ziyili@ustb.edu.cn (Z.L.); whliu@ustb.edu.cn (W.L.)

[2] Beijing Engineering Research Center for Energy Saving and Environmental Protection, University of Science and Technology Beijing, Beijing 100083, China

[3] R&D Center Department, Beijing District Heating Group, Beijing 100026, China; ustbwhh@163.com

* Correspondence: yangx@ustb.edu.cn; Tel.: +86-1062332730

Abstract: Naphthalene (NAP) is a typical gaseous polycyclic aromatic hydrocarbons (PAHs) pollutant that displays toxicological effects on biosystems. Ordered mesoporous carbon has relatively adequate adsorption capacity; however, the attached hydrophilic functional groups were proven to affect the adsorption performance in the presence of moisture. In this paper, trimethylchlorosilane (TMCS) is used to carry out the hydrophobic modification of ordered mesoporous carbon FDU-15, and the adsorption and desorption properties of FDU-15 were studied. Furthermore, the adsorption isotherms of naphthalene on FDU-15 and modified FDU-15 were fitted by L-F equation, and the kinetic parameters of desorption of naphthalene on modified FDU-15 were analyzed based on the method of temperature programming desorption (TPD). The results showed that the micropore volume and specific surface area of FDU-15 were significantly increased after hydrophobically modified by TMCS, and the polar functional groups of the hydrophobically modified FDU-15 were significantly reduced. Furthermore, the adsorption of naphthalene by FDU-15 before and after modification conformed to the L-F equation (R2 > 99%), and the adsorption of naphthalene by modified FDU-5 at low concentration was significantly improved due to the increase of micropores. Based on desorption kinetic performance study of modified FDU-15, it can be seen that the adsorption kinetic characteristics of naphthalene on the modified FDU-15 conform to the mechanical function of the JMA equation. When the mass ratio of TMCs to FDU-15 is 1:10 in the modification process, the pore structure and surface hydrophobicity of the modified FDU-15 reach an excellent balance. At this time, the adsorbent had the optimum desorption performance under experimental conditions, and the desorption activation energy was decreased from 60.98 kJ/mol of FDU-15 to 50.28 kJ/mol.

Keywords: naphthalene; mesoporous carbon; FDU-15; adsorption; desorption kinetics; hydrophobic modification

Citation: Zhao, C.; Liu, Y.; Meng, M.; Li, Z.; Wang, H.; Liu, W.; Yang, X. Research on Adsorption and Desorption Performance of Gas-Phase Naphthalene on Hydrophobic Modified FDU-15. *Processes* **2022**, *10*, 574. https://doi.org/10.3390/pr10030574

Academic Editor: Avelino Núñez-Delgado

Received: 30 January 2022
Accepted: 9 March 2022
Published: 15 March 2022

1. Introduction

Polycyclic aromatic hydrocarbons (PAHs) belong to the class of organic pollutants with continuous pollution to the environment. The studies showed that PAHs possessed three main effects including mutagenic, carcinogenic, and teratogenic to organisms and bioaccumulation ability [1]. Naphthalene was found to be among the volatile PAHs and recently they have attracted attention among the researchers and scholars worldwide for environmental protection purpose [2,3]. Naphthalene is ubiquitously released into the human environment through incomplete combustion processes from industry, households, and natural sources [4]. Motor vehicles, aircraft, fossil fuel combustion, gasoline combustion, industrial plants, forest fires, etc., are listed among the major sources of naphthalene. Therefore, controlling the emission of naphthalene has become an urgent solution to reduce

air pollution and associated risks to human health. Among many naphthalene purification technologies, the adsorption method has become an essential method for removing PAHs due to its high removal efficiency and low energy consumption [5,6].

The adsorption performance of the adsorbent is the core factor for the removal of PAHs by adsorption. Activated carbon has shown a well-developed pore structure and large adsorption capacity for PAHs adsorption [7,8]. However, there are still problems of low mass transfer coefficient and high energy consumption for regeneration [9,10]. Mesoporous molecular sieves have significant advantages in removing PAHs due to their relatively large pore structure, good adsorption capacity, and low energy consumption for desorption [11]. Traditional mesoporous molecular sieves will have many silanols on the surface during the synthesis process. Silicone is a polar group with relatively strong hydrophilicity which makes mesoporous molecular sieves easy to absorb water with a relatively poor hydrothermal stability. This strong absorption property and weak hydrothermal stability have limited application [12].

The mesoporous carbon material was found to have a stable carbon material with hydrophobic properties, and advantages for the adsorption of non-polar PAHs [13]. Yang et al. [1] compared the adsorption and desorption performance of naphthalene on different adsorbents and the result showed that mesoporous carbon has better adsorption performance and lower desorption activation energy than silicon-based mesoporous materials. Liu et al. [14] compared naphthalene adsorption and desorption performance on six carbon materials (FDU-15, CMK-5, CMK-3, two carbon nanotubes and coconut-shell-based activated carbon) in the lab, the result showed ordered mesoporous carbon materials FDU-15 were demonstrated as a superior sorbent with high maximum adsorption capacities (1.13 mmol/g) and low desorption activation energy (62.66 kJ/mol). Similar results shows FDU-15 was proven to be a suitable adsorbent for the adsorption and removal of naphthalene because of low desorption activation energy, the desorption activation energy follows FDU-15 < CMK-5 < CMK-3 [15]. As a good naphthalene removal adsorbent, FDU-15 was structured as a hexagonal pore arrangement with a primary mesopore size of 2.5–7.5 nm.

However, mesoporous carbon materials such as FDU-15 are obtained by carbonization [16,17]. Mesoporous adsorbents such as FDU-15 will participate in some polar functional groups such as oxygen-containing functional groups during the carbonization process [18,19]. These polar functional groups enhance the competitive adsorption properties of moisture on carbon materials and seriously affect the adsorption of other pollutants [20]. Hydrophobically modify carbon materials is an effective way to improve the adsorption capacity in the presence of moisture [20]. Furthermore, the use of silane to modify the adsorbent was also found to be effective method for adsorbent hydrophobicity improvement. Kim et al. [21] and Li et al. [22] use polydimethylsiloxane (PDMS) to hydrophobic modify activated carbon materials, increasing the selectivity and adsorption capacity of VOC in the presence of moisture. Li et al. [23] modified activated carbon with trimethylchlorosilane (TMCS) to improve the hydrophobic property. At 90% humidity, the adsorption capacity of TMCS modified activated carbon decreased only 9% compared with the dry gas, much better than original activated carbon. Li et al. [24] modified SBA-15 with TMCS and phenyldimethyldichlorosilane(PDMCS), and the results showed a good hydrophobicity. Wang et al. [25] used TMCS to modify SBA-15 hydrophobically, and SBA-15-TMCS had better adsorption performance than activated carbon in the adsorption of n-hexane and 93# gasoline.

However, there is few studies on the hydrophobic modification of FDU-15 and the adsorption and desorption performance of polycyclic aromatic hydrocarbons after hydrophobic modification. Current work will hydrophobically modify ordered mesoporous carbon FDU-15 using TMCS. The adsorption and desorption performance of naphthalene on FDU-15 and modified FDU-15 were studied. This study will provide some technical support for the hydrophobic modification of adsorbents to improve the adsorption and desorption performance of PAHs and VOCs.

2. Experimental Part

2.1. Adsorbents and Characterization

The adsorbents used in the experiments were FDU-15 mesoporous carbon (bought from Zibo Huatong Chemical Reagent Co., Ltd., Zibo, China) and modified FDU-15. The modified FDU-15 was hydrophobically modified through post-implantation method. Since TMCS is very easy to hydrolyze ginseng hydrochloric acid, toluene was used to dissolve TMCS in this experiment. First, FDU-15 was dried at 100 °C for 10 h to remove adsorbed water on its surface. Then, a certain proportion of TMCS and FDU-15 was added to a flat-bottomed flask containing 100 mL of toluene according to a certain mass ratio, stirred, and heated under reflux for 6 h at 30 °C to avoid the toluene volatilization into the air. At every sample modification experiment, the weight of FDU-15 added to the reaction is 500 mg. After the reaction, the solution was subjected to suction filtration to obtain the adsorbent powder, washed with alcohol 4 to 6 times. Then, adsorbent powder obtained after suction filtration was placed in a constant temperature and humidity test box and dried at 120 °C for 6 h. In this study, the mass ratios of TMCS and FDU-15 were 1:20, 1:10, and 3:20, and the modified samples were marked as TMCS-FDU-15n, where n represented the mass ratio of TMCS to FDU-15.

The adsorption–desorption experiments of Ar (87K) were carried out on the adsorbent samples by Autosorb-1 automatic surface area and pore size distribution analyzer (Quantachrome Instruments, Boynton Beach, FL, USA). The specific surface area S_{BET} of the sample is calculated by the BET (Brunauer–Emmett–Teller). Equation to calculate the isotherm data of the relative pressure was between 0.05 and 0.30. The pore size distribution is calculated according to the NLDFT (Non-local density functional theory) model. The total pore volume is calculated from the adsorption amount when the relative pressure (P/P0) is 0.99.

The modified samples were analyzed by ALPHA Fourier transform infrared spectrometer from Bruker, Germany. During the detection of the loading of hydrophilic groups on the adsorbent surface, the scanning range was 4000–400 cm^{-1}, the resolution was 4 cm^{-1}, and the number of scanning was 16 times, whereas potassium bromide powder tableting was used as the background. Mass ratio of adsorbent to potassium bromide was 1:100.

2.2. Adsorption Experiment

2.2.1. Adsorption Experiment Device

The experimental device that was used for naphthalene is shown on Figure 1 and it is mainly composed of a gas-phase naphthalene generation unit, adsorption column, an flame ionization detector-gas chromatography (FID-GC), detection device, and a pipeline insulation system. The gas-phase naphthalene is formed by the sublimation of crystals in a quartz tube, and the amount of naphthalene was about 50 mg. The intake concentration is controlled by changing water bath temperature (−10~60 °C) of the low-temperature thermostat. The carrier gas (high-purity helium) carried gas-phase naphthalene into the adsorption test system with a flow rate of 10 $mL \cdot min^{-1}$ was employed. Naphthalene concentration was detected by the FID method. After the pipeline is purged, gas stream carrying gas-phase naphthalene is passed through the adsorption bypass. When the FID detection value became stable, naphthalene gas was passed into the adsorption bed for adsorption experiments, and the experimental values were recorded. The adsorption temperature was set as 125 ± 0.1 °C and the adsorption column was a quartz glass tube with an inner diameter of 3 mm and a length of 125 mm. The adsorption column was placed in a chromatograph furnace. To ensure sufficient bed length to achieve plug flow, the adsorbent was mixed and filled with 2 to 4 mg of adsorbent and about 1.0 g of quartz sand (80 to 100 mesh) mixture. A blank test verified the adsorption capacity of inert quartz sand to naphthalene was found to be negligible. To avoid naphthalene condensing in the pipeline, the pipeline was wrapped with heating tape between the naphthalene generating device's outlet and the chromatograph's inlet.

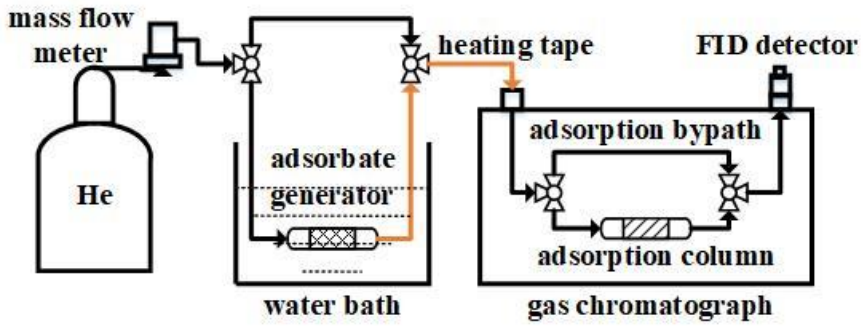

Figure 1. Schematic diagram of experiment system for Nap adsorption.

2.2.2. Calculation of Adsorption Capacity

The equilibrium adsorption capacity of the adsorbent is calculated according to Equation (1) [26]:

$$q_0 = \frac{Q(C_0 t_f - \int_0^{t_f} C(t)dt)}{m} \quad (1)$$

where, q_0 is the equilibrium adsorption capacity of naphthalene, mg·mg^{-1}; Q is the gas flow rate, m^3·min^{-1}; C_0 is the inlet gas phase naphthalene concentration, the naphthalene concentration is the saturated concentration of naphthalene at the water bath temperature T, mg·m^{-3}; t_f is the breakthrough time, min; $C(t)$ is the concentration of naphthalene in the outlet gas phase at time t, mg·m^{-3}; and m is the mass of the adsorbent, mg. The saturated vapor pressure and saturated concentration of naphthalene in the gas phase can be calculated [27].

2.3. Desorption Experiment

2.3.1. Desorption Experimental Method

Desorption characteristics are significant in terms of selecting appropriate sorbents to remove or recycle PAHs during chemical engineering processes. In this study, thermogravimetric analysis (TGA) [28] was employed to study the desorption kinetics of naphthalene on the adsorbent. During the experiment, 15 mL of methanol solution of naphthalene with a concentration of 0.2 mol·L^{-1} was prepared. An appropriate amount of adsorbent was poured into the solution and left at room temperature for 12 h. Then, the naphthalene-loaded adsorbent samples were taken out and dried at 333 K for 2 h. A sample of 10 ± 1 mg was taken in each experiment, and thermal desorption experiments were carried out at three heating rates (β = 8, 16, 20 K·min^{-1}). The experimental instrument was Q50 thermogravimetric analyzer from Worcester, USA.

2.3.2. Determination of Activation Energy

To obtain the desorption activation energy of naphthalene on the adsorbent, the KAS (Kissinger–Akahira–Sunose) method was used to analyze and calculate the desorption activation energy of naphthalene on the mesoporous material. The expression is as follows [29]:

$$\ln(\frac{\beta}{{T_p}^2}) = \ln\frac{AR}{E_a g(\alpha)} - \frac{E_a}{RT_p} \quad (2)$$

where, α is the desorption conversion rate, which is a constant, $g(\alpha)$ is the desorption mechanism function, and T_p is the peak temperature on the TPD curve. This formula can be regarded as ln ($\beta/{T_p}^2$). For a linear function of $1/T_p$ the slope of the straight line is $-E_a/T_p$ from which the desorption activation energy E_a can be obtained.

2.3.3. Determining the Probable Mechanism Function

The most probable mechanism function was determined by combining E_a calculated by the KAS and master curve method. The obtained probable mechanism function $g(\alpha)$ was substituted into the KAS equation to obtain the pre-exponential factor, so as to obtain accurate desorption. The common desorption mechanism function expressions are shown in Table 1.

Table 1. Common mechanism function expressions.

Symbol	Model	Differential Form	Integral Form
	Diffusion Model		
D1	one-dimensional diffusion	$(1/2)\alpha^{-1}$	$\alpha 2$
D2	two-dimensional diffusion	$[-\ln(1-\alpha)]^{-1}$	$\alpha + (1-\alpha)\ln(1-\alpha)$
D3	3D Diffusion (ZLT Equation)	$(3/2)(1-\alpha)^{4/3}\,[(1-\alpha)^{-1/3}-1]^{-1}$	$[(1-\alpha)-1/3-1]^2$
	Nucleation model		
A_m	Random Nucleation and Nucleation Growth (JMA(Johnson-Mehl-Arvami) equation; parameters m = 4, 3, 2, 3/2, 4/3, 1, 2/3, 1/2, 1/3, 1/4)	$m(1-\alpha)[-\ln(1-\alpha)]^{1-1/m}$	$[-\ln(1-\alpha)]^{1/m}$
	geometric shrinkage model		
R_2	Phase boundary reaction (cylindrical symmetry)	$2(1-\alpha)^{1/2}$	$1-(1-\alpha)^{1/2}$
R_3	Phase boundary reaction (spherical symmetry)	$3(1-\alpha)^{2/3}$	$1-(1-\alpha)^{1/3}$
	Reaction series model		
$F_1(A_1)$	First-order	$1-\alpha$	$-\ln(1-\alpha)$
F_2	Second order	$(1-\alpha)^2$	$(1-\alpha)^{-1}-1$
F_3	Third order	$(1-\alpha)^3$	$0.5\,[(1-\alpha)^{-2}-1]$

The integral form of the thermal analysis kinetic Equation [26] is as follows.

$$g(\alpha) = \frac{A \bullet E_a}{\beta \bullet R} P(x) \tag{3}$$

where $P(x)$ is the integral function of temperature, $x = E_a/(R \bullet T)$ is the value of x corresponding to the conversion rate α, and T is the temperature corresponding to the conversion rate α, K. For the desorption process that can be described by a single kinetic mechanism function, $A \bullet E_a/(\beta \bullet R)$ in Equation (3) is a constant, and for the most probable mechanism function:

$$\frac{g(\alpha)}{g(0.5)} = \frac{P(x)}{P(0.5)} \tag{4}$$

The value of $P(x)$ can be obtained from the empirical formula [30]:

$$P(x) = \frac{e^{-x}}{x(1.00198882x + 1.87391198)} \tag{5}$$

The common mechanistic functions are list in Table 1.

3. Experimental Results and Discussion

3.1. Characterization of Adsorbents

3.1.1. Analysis of Channel Characteristics

Figure 2 shows the pore size distribution of FDU-15 before and after modification. It determined that both FDU-15 and TMCS-FDU-$15_{1\text{-}20}$ had only mesoporous structures, while TMCS-FDU-$15_{1\text{-}10}$ and TMCS-FDU-$15_{3\text{-}20}$ showed a small amount of microporous structure after modification. Table 1 shows the specific surface area and the pore volume in different pore size ranges of FDU-15 and modified FDU-15. The results also showed that the specific surface area of FDU-15 increased after modification. When the mass ratio of TMCS and FDU-

15 is 1:20, the specific surface area reached a maximum of 1733 m^2/g. The specific surface area gradually decreased to 1237 m^2/g when the ratio of TMCS: FDU-15 was 3:20. The pore volume result in Table 2 shows, the pore volume of FDU-15 decreased gradually with increase of input amount of modifier TMCS during the modification process. Additionally, the microporous structure in FDU-15 began to appear with increase of modifier TMCS input. When TMCS: FDU-15 was 1:10, the micropore pore volume reached the highest value of 0.09 cc/g. This was due to insufficient amount of TMCS added, the molecules of TMCS only occupy part of the mesoporous channels with larger diameters and form a new mesoporous structure, which leads to an increase in the specific surface area of adsorbent after modification. The occupancy of modified TMCS in the pores may lead to blockage of a part of the pores, thereby reducing the pore volume. When TMCS increased, TMCS was further deposited in the newly created channels, and a microporous structure appeared. However, with the further deposition of TMCS, the micropores were further blocked, resulting in a decrease of micropore volume.

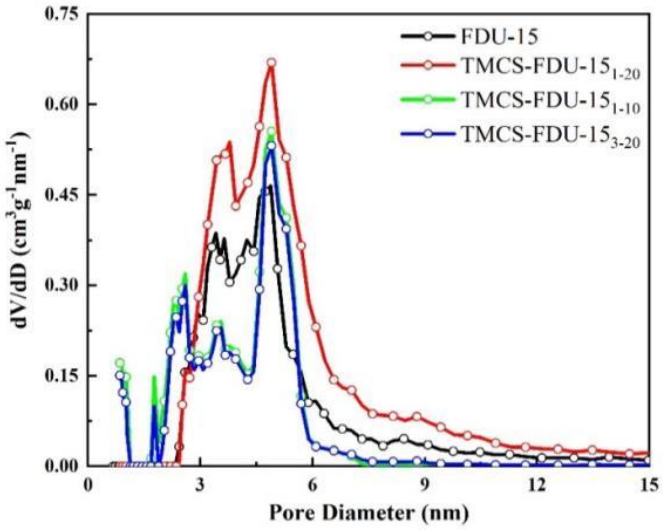

Figure 2. Pore size distribution of FDU-15 and modified FDU-15.

Table 2. Pore structure parameters of FDU-15 and modified FDU-15.

Sample	S_{BET} (m^2/g)	V_p ($cm^3 \cdot g^{-1}$)	V_{micro} ($cm^3 \cdot g^{-1}$)	V_{meso} ($cm^3 \cdot g^{-1}$)	*dp* (nm)
FDU-15	1149	1.39	0.00	1.39	4.9
TMCS-FDU-15 $_{1\text{-}20}$	1733	1.25	0.00	1.25	4.9
TMCS-FDU-15 $_{1\text{-}10}$	1382	1.14	0.09	1.05	4.9
TMCS-FDU-15 $_{3\text{-}20}$	1237	1.06	0.06	1.00	4.9

Through the result of pore structure of modified FDU-15, it can be indicated that in the process of hydrophobic modification of mesoporous carbon materials by TMCS, adding an appropriate amount of TMCS can increase the pore diversity of mesoporous carbon materials, and increase the micropore volume and specific surface area.

3.1.2. FTIR Analysis

Figure 3 shows fourier transform infrared spectroscopy (FTIR) results of FDU-15 and modified FDU-15. The results indicated that the stretching vibration peak of -OH around 3700 cm^{-1} [31] gradually decreased with increase of the amount of TMCS on FDU-15. As a result, the hydrophobicity of the adsorbent has been effectively improved after being modified by TMCS. The peak at 2350 cm^{-1} may be due to the adsorption of CO_2 [32]. CO_2 adsorption peaks may be associated with the carbon dioxide adsorbent in an air

environment [33]. It was noticed that the increase of the amount of modifier TMCS with the adsorption peak of CO_2 gradual weakened. It can be concluded that the stronger the surface polarity of the adsorbent, the stronger the adsorption capacity of CO_2 on the adsorbent. From the FTIR of the adsorbent, the peaks at 3700 cm^{-1} and 2350 cm^{-1} are both gradually slowing downward trends and disappearing as the mass of the modifier increased. The result shows the polarity of the adsorbent surface weakens with the quality of the modifier increased. This indicated that the hydrophobicity of the FDU-15 increased with the rise of the modifier TMCS.

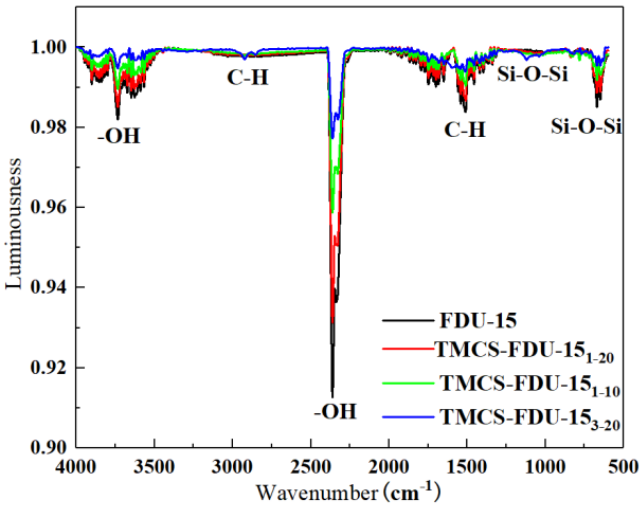

Figure 3. FTIR spectra of FDU-15 and modified FDU-15.

3.2. Adsorption Performance Analysis

Figure 4 shows the adsorption isotherms of gas-phase naphthalene on FDU-15 and modified FDU-15 As can be seen from Figure 4, the adsorption isotherms of FDU-15 and modified FDU-15 are all type-I isotherms. The isotherms type indicated that the adsorption equilibrium mechanism of naphthalene in this concentration range was dominated by micropore filling and monolayer surface adsorption. The adsorption isotherms can be fitted by the L-F Equation [34]. Table 3 shows adsorption isotherms equation parameters of FDU-15 and modified FDU-15 by the L-F isotherm equation. The fitting result shows the L-F model is very suitable for describing the adsorption of naphthalene on FDU-15 and modified FDU-15 (R^2 > 99%).

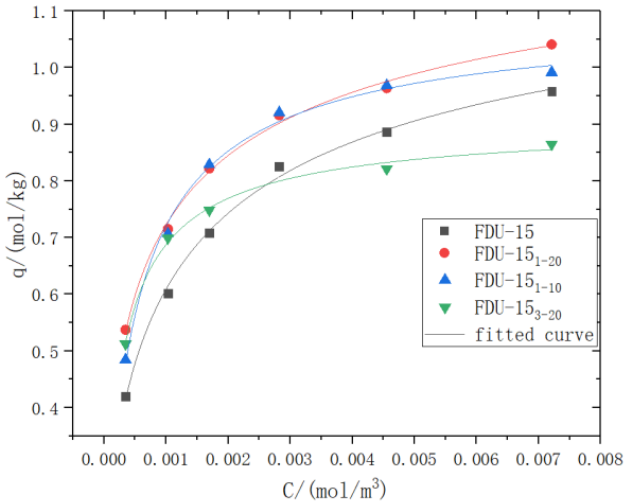

Figure 4. Adsorption isotherms of Nap on FDU-15 and modified FDU-15.

Table 3. Fitting results of Nap adsorption isotherms on FDU-15 and modified FDU-15.

Adsorbent	q_m	b	n	R^2/%
FDU-15	1.283	59.865	0.607	99.5
TMCS-FDU-$15_{1\text{-}20}$	1.354	46.373	0.536	99.5
TMCS-FDU-$15_{1\text{-}10}$	1.102	704.934	0.857	99.2
TMCS-FDU-$15_{3\text{-}20}$	0.910	895.218	0.821	99.2

Figure 4 also showed that the adsorption capacity of FDU-15 in the modified adsorbent changed accordingly. For instance, when the concentration of naphthalene was less than 2.6 mmol/m^3 (330 mg/m^3), the adsorption capacity of FDU-15 modified by TMCS was higher than that of FDU-15. The concentration of naphthalene on common flue gas was 100~200 mg/m^3. This indicated that the modified FDU-15 by TMCS has an effective adsorption capacity for naphthalene in the flue gas.

The adsorption capacity of naphthalene on TMCS modified FDU-15 increased was due to the fact that the modified FDU-15 has more microporous structures. At a low concentrations, naphthalene first fills the micropores due to the micropore filling effect, and then adsorbs in the pores. However, when the amount of TMCS modification became large, the pores of the adsorbent also become further blocked, which resulting in a lower adsorption capacity of FDU-$15_{3\text{-}20}$ than that of unmodified FDU-15 at a concentration higher than 2.6 mmol/m^3. It is also noted from the figure that TMCS-FDU-$15_{1\text{-}20}$ has a large of specific surface area and pore volume compared toTMCS-FDU-$15_{1\text{-}10,}$ Thus, the adsorption capacity for naphthalene on FDU-$15_{1\text{-}10}$ was slightly higher. From the adsorption capacity result of modified FDU-15, it can be inferred that the carbon materials with developed micropore structure has good naphthalene adsorption capacity at low concentration. It is suitable for removal of low concentration of gas phase naphthalene from flue gas.

3.3. Desorption Performance Analysis

3.3.1. Desorption Curve Analysis

Figure 5a,b are the TG and DTG curves of naphthalene desorption of each sample when the heating rate was 8 K/min, 16 K/min and 20 K/min, respectively. Figure 5a demonstrated that the desorption the amount of naphthalene at different elevated desorption temperatures were almost similar. This indicated that the desorption of naphthalene finished at the corresponding temperature.

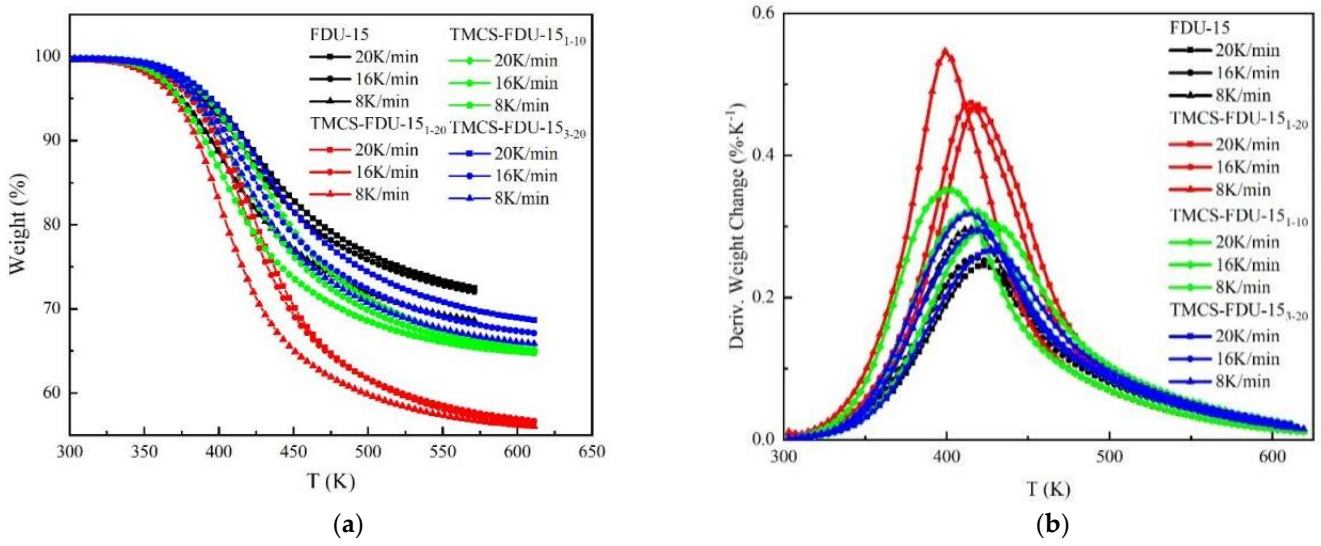

(**a**) (**b**)

Figure 5. Desorption curve of naphthalene on FDU-15 before and after modification, (**a**) TG curve, and (**b**) DTG curve.

Based on DTG curves of naphthalene desorption in Figure 5b, each DTG curve has only one desorption rate peak under different heating rates. The peak temperature is between 400 and 450 K. With the increase of modifier addition, the peak temperature showed a trend of gradual increase. For the same adsorbent, the increase of heating rate, the peak temperature of the DTG curve gradually rose. Among different adsorbents, the overall peak temperature followed TMCS-FDU-$15_{3\text{-}20}$ > TMCS-FDU-$15_{1\text{-}10}$ > TMCS-FDU-$15_{1\text{-}20}$ ≈ FDU-15.

The difference of desorption peaks is mainly due to the combined effect of the pore size and the hydrophobicity of the adsorbent. The pore size of the adsorbent became smaller with the increase of the amount of TMCS. When the pore size of the adsorbent becomes smaller, the stronger the interaction between the adsorbent and the naphthalene molecule [5], the higher the required temperature in the desorption process needed. However, with the increase of the amount of TMCS, the polar groups on the adsorbent surface gradually decreased. This will weaken the adsorption force of naphthalene on the adsorbent surface. Therefore, when the amount of TMCS for FDU-15 modification is small, despite of interaction between the adsorbent and adsorbate molecules which is enhanced, but the micropores barely increased. The difference between desorption peak temperature of TMCS-FDU-$15_{1\text{-}20}$ and FDU-15 was negligeable.

3.3.2. Desorption Kinetics Parameter Calculation

According to the KAS equation of Formula (2), the desorption activation energy Ea and lnA of each sample were calculated, and the results were shown in Table 4. The desorption activation energy of naphthalene on four adsorbents follows TMCS-FDU-$15_{1\text{-}10}$ < TMCS-FDU-$15_{1\text{-}20}$ ≈ FDU-15 < TMCS-FDU-$15_{3\text{-}20}$. When the mass ratio of TMCS and FDU-15 was 1:10, the desorption activation energy of naphthalene on the modified adsorbent was the lowest, which was 50.28 kJ·mol^{-1}.

Table 4. Three factors of desorption kinetics of Nap on FDU-15 and modified FDU-15.

Desorption Kinetics Three Factors	Adsorbent			
	FDU-15	**TMCS-FDU-$15_{1\text{-}20}$**	**TMCS-FDU-$15_{1\text{-}10}$**	**TMCS-FDU-$15_{3\text{-}20}$**
Model	$A_{1/3}$	$A_{1/2}$	$A_{1/2}$	$A_{1/4}$
E_a (kJ/mol)	60.98	60.59	50.28	95.3
ln A (min^{-1})	11.00	15.81	12.48	20.46

Substitute the value Ea of the desorption activation energy obtained according to the KAS equation into the Formula (4), the relationship between α and $g(\alpha)/g(0.5)$ experimental results can be obtained. The desorption mechanism function of naphthalene on FDU-15, TMCS-FDU-$15_{1\text{-}20}$, TMCS-FDU-$15_{1\text{-}10}$ and TMCS-FDU-$15_{3\text{-}20}$ are $A_{1/3}$, $A_{1/2}$, $A_{1/2}$ and $A_{1/4}$, respectively. Figure 6 gave the comparison of the experiment result with the theoretical value curves, which were calculated by different mechanism functions. The obtained results showed the desorption mechanism functions of naphthalene on FDU-15 and modified FDU-15 fit very well. The desorption mechanism functions of naphthalene on FDU-15 and modified FDU-15 were all in accordance with the JMA equation in the random nucleation growth model, which was characterized by the formation of nuclei and the control of growth rate. The desorption mechanism function of naphthalene on FDU-15 was $A_{1/3}$, whereas desorption mechanism function of naphthalene on TMCS-FDU-$15_{1\text{-}20}$ and TMCS-FDU-$15_{1\text{-}10}$ was $A_{1/2}$. The mechanism function for desorption on FDU-$15_{3\text{-}20}$ was $A_{1/4}$.

Substituting the desorption activation energy E_a and the mechanism function into the intercept formula of the KAS equation, the pre-exponential factor in the three factors of desorption kinetics of naphthalene on FDU-15 and modified FDU-15 can be obtained, the result was illustrated in Table 4. The pre-exponential factors lnA of FDU-15, TMCS-FDU-$15_{1\text{-}20}$, TMCS-FDU-$15_{1\text{-}10}$, and TMCS-FDU-$15_{3\text{-}20}$ were 11, 15.81, 12.48, and 20.46, respectively.

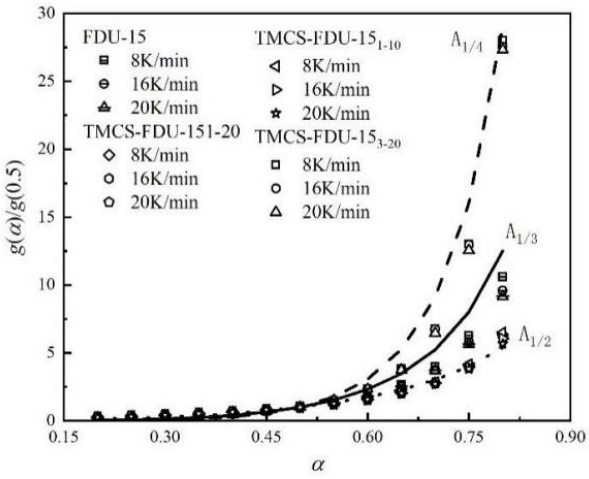

Figure 6. Comparison of standard and experimental master plots of desorption mechanism function for naphthalene on FDU-15.

Table 4 showed that the desorption kinetic models of naphthalene on the four adsorbents all satisfy the JMA rate equation based on the nucleation growth model $g(\alpha) = [-\ln(1-\alpha)]^{1/m}$. This equation can describe the reaction kinetics in the phase transition and decomposition process [35,36], where the exponent was closely related to the reaction form. When 1/m is greater than 1, the reaction mainly forms nuclei and growth rate control.

The desorption activation energy of naphthalene on the four FDU-15 in Table 4 shows that the desorption activation energy of FDU-15-TMCS$_{1-20}$ and FDU-15 are almost the similar. This was due to the fact that when the amount of TMCS added was small (the mass ratio of TMCS: FDU-15 is 1:20), the pore structure of the adsorbent had little change after modification, which hardly affects the desorption and diffusion process of naphthalene on the adsorbent. When TMCS added increased slightly (mass ratio of TMCS: FDU-15 is 1:10), the microporous of adsorbent was significantly increased. In contrast, the polar functional groups of the surface of the adsorbent were significantly reduced, and the hydrophobic functional group grew. Thus, the adsorption energy of naphthalene slightly decreased, while the micro-mesoporous interconnected structure formed after the modification of FDU-15, which was beneficial to desorption and mass transfer [37,38]. However, with the further increase of the amount of TMCS, the pore structure of the adsorbent may be blocked. In this case, the desorption process was not conducive to the diffusion of naphthalene molecules, so the desorption activation energy of TMCS-FDU-15$_{3-20}$ is higher than that of FDU-15 [38].

Based on the analysis results of FTIR, pore size distribution, and adsorption and desorption performance, it was determined that when the mass ratio of TMCS and FDU-15 reaches a specific value, the modified FDU-15 can achieve a balance in the surface structure and functional groups of the adsorbent. At this time, naphthalene's adsorption and desorption performance can reach a relatively optimal value. In this study, when the mass ratio of TMCS to FDU-15 was 1:10, the modified FDU-15 exhibited the best adsorption and desorption properties for naphthalene.

4. Conclusions

(1) Hydrophobic modification of FDU-15 adsorbent with trimethylchlorosilane (TMCS) can increase the content of micropores and specific surface area of FDU-15. In this study, the specific surface area of modification using FDU-15 followed TMCS-FDU-15$_{1-20}$ > TMCS-FDU-15$_{1-10}$ > TMCS-FDU-15$_{3-20}$ > FDU-15.

(2) Hydrophobic modification of FDU-15 with an appropriate amount of TMCS was beneficial to improve the adsorption performance of the adsorbent for naphthalene at low concentrations. Under the experimental conditions studied in this paper,

TMCS-FDU-$15_{1\text{-}20}$ and TMCS-FDU-$15_{1\text{-}10}$ modified with a small amount of TMCS can significantly improve the naphthalene adsorption capacity at low concentrations.

(3) When the mass ratio of TMCS and FDU-15 was 1:10, the adsorbent's pore structure and surface hydrophobicity can reach an optimal balance. Under this condition, the desorption activation energy of the adsorbent for naphthalene decreased from 60.98 kJ/mol of the raw FDU-15 and reduced to a minimum of 50.28 kJ/mol.

(4) Based on experiment conditions, the desorption mechanism functions of naphthalene on FDU-15 and modified FDU-15 were in accordance with the JMA equation, which is characterized by the formation of nuclei and the rate of growth.

Author Contributions: Conceptualization, C.Z. and Y.L.; methodology, M.M. and H.W.; validation, Z.L. and W.L.; formal analysis, C.Z. and X.Y.; investigation, C.Z.; writing—original draft preparation, C.Z. and Z.L.; writing—review and editing, X.Y.; supervision, Y.L.; project administration, X.Y. All authors have read and agreed to the published version of the manuscript.

Funding: This research was funded by supported by the Fundamental Research Funds for the Central Universities, grant number FRF-GF-19-005A and FRF-BD-20-09A.

Institutional Review Board Statement: Not applicable.

Informed Consent Statement: Not applicable.

Conflicts of Interest: The authors declare no conflict of interest.

References

1. Yang, X.; Li, Z.; Liu, Y.; Xing, Y.; Wei, J.; Yang, B.; Tsai, C.J. Research progress of gaseous polycyclic aromatic hydrocarbons purification by adsorption. *Aerosol Air Qual. Res.* **2019**, *19*, 911. [CrossRef]
2. Mukwevho, N.; Gusain, R.; Fosso-Kankeu, E.; Kumar, N.; Waanders, F.; Ray, S.S. Removal of naphthalene from simulated wastewater through adsorption-photodegradation by ZnO/Ag/GO nanocomposite. *J. Ind. Eng. Chem.* **2020**, *81*, 393. [CrossRef]
3. Wu, Z.; Liu, P.; Wu, Z.; Cravotto, G. In Situ Modification of Activated Carbons by Oleic Acid under Microwave Heating to Improve Adsorptive Removal of Naphthalene in Aqueous Solutions. *Processes* **2021**, *9*, 391. [CrossRef]
4. Preuss, R.; Angerer, J.; Drexler, H. Naphthalene-an environmental and occupational toxicant. *Int. Arch. Occup. Environ. Health* **2003**, *76*, 556. [CrossRef] [PubMed]
5. Yang, X.; Zhang, C.; Jiang, L.; Li, Z.; Liu, Y.; Wang, H.; Yang, R.T. Molecular simulation of naphthalene, phenanthrene, and pyrene adsorption on MCM-41. *Int. J. Mol. Sci.* **2019**, *20*, 665. [CrossRef]
6. Dowaidar, A.M.; El-Shahawi, M.S.; Ashour, I. Adsorption of polycyclic aromatic hydrocarbons onto activated carbon from non-aqueous media: The Influence of the Organic Solvent Polarity. *Sep. Sci. Technol.* **2007**, *42*, 3609. [CrossRef]
7. Mastral, A.M.; García, T.; Callén, M.S.; Navarro, M.V.; Galban, J. Assessement of phenanthrene removal from hot gas by porous carbons. *Energy Fuels* **2001**, *15*, 1. [CrossRef]
8. Li, F.; Chen, J.; Hu, X.; He, F.; Bean, E.; Tsang, D.C.; Gao, B. Applications of carbonaceous adsorbents in the remediation of polycyclic aromatic hydrocarbon-contaminated sediments: A review. *J. Clean. Prod.* **2020**, *255*, 120263. [CrossRef]
9. Liu, Y.; Li, Z.; Yang, X.; Xing, Y.; Tsai, C.; Yang, Q.; Yang, R.T. Performance of mesoporous silicas (MCM-41 and SBA-15) and carbon (CMK-3) in the removal of gas-phase naphthalene: Adsorption capacity, rate and regenerability. *Rsc Adv.* **2016**, *6*, 21193–21203. [CrossRef]
10. Kosuge, K.; Kubo, S.; Kikukawa, N.; Takemori, M. Effect of pore structure in mesoporous silicas on VOC dynamic adsorption/desorption performance. *Langmuir* **2007**, *23*, 3095. [CrossRef]
11. Loussala, H.M.; Han, S.; Feng, J.; Sun, M.; Feng, J.; Fan, J.; Pei, M. Mesoporous silica hybridized by ordered mesoporous carbon for in-tube solid-phase microextraction. *J. Sep. Sci.* **2020**, *43*, 3655–3664. [CrossRef] [PubMed]
12. Zhao, X.S.; Lu, G.Q.; Whittaker, A.K.; Millar, G.J.; Zhu, H.Y. Comprehensive study of surface chemistry of MCM-41 using ^{29}Si CP/MAS NMR, FTIR, Pyridine-TPD, and TGA. *J. Phys. Chem. B* **1997**, *101*, 6525. [CrossRef]
13. Li, Z.; Liu, Y.; Yang, X.; Xing, Y.; Tsai, C.J.; Meng, M.; Yang, R.T. Performance of mesoporous silicas and carbon in adsorptive removal of phenanthrene as a typical gaseous polycyclic aromatic hydrocarbon. *Microporous Mesoporous Mater.* **2017**, *239*, 9. [CrossRef]
14. Liu, Y.; Zhao, C.; Li, Z.; Meng, M.; Yang, X.; Bian, W.; Yang, R.T. Adsorption and desorption of gaseous naphthalene on carbonaceous sorbents: Insights into advantageous pore sizes and morphologies. *J. Clean. Prod.* **2021**, *314*, 127905. [CrossRef]
15. Li, Z.Y.; Liu, Y.S.; Yang, X.; Meng, M.M.; Zhang, C.Z. Study of naphthalene desorption properties on typical mesoporous. *J. Eng. Thermophys.* **2017**, *38*, 1478.
16. Meng, Y.; Gu, D.; Zhang, F.; Shi, Y.; Yang, H.; Li, Z.; Zhao, D. Ordered mesoporous polymers and homologous carbon frameworks: Amphiphilic surfactant templating and direct transformation. *Angew. Chem. Int. Ed.* **2005**, *44*, 7053–7059. [CrossRef]

17. Ndamanisha, J.C.; Guo, L. Ordered mesoporous carbon for electrochemical sensing: A review. *Anal. Chim. Acta* **2012**, *747*, 19–28. [CrossRef]
18. Wu, Z.; Webley, P.A.; Zhao, D. Comprehensive study of pore evolution, mesostructural stability, and simultaneous surface functionalization of ordered mesoporous carbon (FDU-15) by wet oxidation as a promising adsorbent. *Langmuir* **2010**, *26*, 10277–10286. [CrossRef]
19. Wang, Y.; Zhang, H.; Wang, G.; Liu, L.; Yu, Y.; Chen, A. Preparation of mesoporous carbon from biomass for heavy metal ion adsorption. *Fuller. Nanotub. Carbon Nanostruct.* **2017**, *25*, 102–108. [CrossRef]
20. Guo, X.; Li, X.; Gan, G.; Wang, L.; Fan, S.; Wang, P.; Liu, S. Functionalized Activated Carbon for Competing Adsorption of Volatile Organic Compounds and Water. *ACS Appl. Mater. Interfaces* **2021**, *13*, 56510–56518. [CrossRef]
21. Kim, K.-D.; Park, E.J.; Seo, H.O.; Jeong, M.-G.; Kim, Y.D.; Lim, D.C. Effect of Thin Hydrophobic Films for Toluene Adsorption and Desorption Behavior on Activated Carbon Fiber Under Dry and Humid Conditions. *Chem. Eng. J.* **2012**, *200–202*, 133–139. [CrossRef]
22. Li, X.; Zhang, L.; Yang, Z.; He, Z.; Wang, P.; Yan, Y.; Ran, J. Hydrophobic Modified Activated Carbon Using PDMS for the Adsorption of VOCs in Humid Condition. *Sep. Purif. Technol.* **2020**, *239*, 116517–116527. [CrossRef]
23. Li, Z.; Jin, Y.; Chen, T.; Tang, F.; Cai, J.; Ma, J. Trimethylchlorosilane Modified Activated Carbon for the Adsorption of VOCs at High Humidity. *Sep. Purif. Technol.* **2021**, *272*, 118659. [CrossRef]
24. Li, H.Y.; Guo, J.F. Study on mesoporous SBA-15 modified by organochlorosilane and its hydrophobicity. *Chem. World* **2011**, *52*, 389.
25. Wang, H.; Wang, T.; Han, L.; Tang, M.; Zhong, J.; Huang, W.; Chen, R. VOC adsorption and desorption behavior of hydrophobic, functionalized SBA-15. *J. Mater. Res.* **2016**, *31*, 516. [CrossRef]
26. Li, Z.Y.; Liu, Y.S.; Yang, X.; Xing, Y.; Yang, Q.; Yang, R.T. Adsorption thermodynamics and desorption properties of gaseous polycyclic aromatic hydrocarbons on mesoporous adsorbents. *Adsorption* **2017**, *23*, 361. [CrossRef]
27. Delle Site, A. The vapor pressure of environmentally significant organic chemicals: A review of methods and data at ambient temperature. *J. Phys. Chem. Ref. Data* **1997**, *26*, 157. [CrossRef]
28. Li, Z.; Liu, Y.; Yang, X.; Xing, Y.; Tsai, C.; Wang, Z.; Yang, R.T. Desorption of polycyclic aromatic hydrocarbons on mesoporous sorbents: Thermogravimetric experiments and kinetics study. *Ind. Eng. Chem. Res.* **2016**, *55*, 1183. [CrossRef]
29. Janković, B.; Adnađević, B.; Jovanović, J. Application of model-fitting and model-free kinetics to the study of non-isothermal dehydration of equilibrium swollen poly (acrylic acid) hydrogel: Thermogravimetric analysis. *Thermochim. Acta.* **2007**, *452*, 106. [CrossRef]
30. Wanjun, T.; Yuwen, L.; Xi, Y.; Cunxin, W. Kinetic studies of the calcination of ammonium metavanadate by thermal methods. *Ind. Eng. Chem. Res.* **2004**, *43*, 2054. [CrossRef]
31. Salonen, J.; Lehto, V.P.; Laine, E. Thermal oxidation of free-standing porous silicon films. *Appl. Phys. Lett.* **1997**, *70*, 637. [CrossRef]
32. Stevens, R.W., Jr.; Siriwardane, R.V.; Logan, J. In situ fourier transform infrared (FTIR) investigation of CO_2 adsorption onto zeolite materials. *Energy Fuels* **2008**, *22*, 3070. [CrossRef]
33. Rege, S.U.; Yang, R.T. A novel FTIR method for studying mixed gas adsorption at low concentrations: H_2O and CO_2 on NaX zeolite and γ-alumina. *Chem. Eng. Sci.* **2001**, *56*, 3781. [CrossRef]
34. Yang, X.; Epiepang, F.E.; Li, J.; Wei, Y.; Liu, Y.; Yang, R.T. Sr-LSX zeolite for air separation. *Chem. Eng. J.* **2019**, *362*, 482. [CrossRef]
35. Li, Z.; Liu, Y.; Yang, X.; Wang, Z.; Yang, Q.; Yang, R.T. Desorption kinetics of naphthalene and acenaphthene over two activated carbons via thermogravimetric analysis. *Energy Fuels* **2015**, *29*, 5303. [CrossRef]
36. Drewien, C.A.; Tallant, D.R.; Eatough, M.O. Thermal stability and decomposition kinetics of $Li_2Al_4CO_3(OH)_{12}{\cdot}3H_2O$. *J. Mater. Sci.* **1996**, *31*, 4321. [CrossRef]
37. Li, Z.Y.; Liu, Y.S.; Jiang, L.J. Research progress on adsorption purification technology of gaseous polycyclic aromatic hydrocarbons. *Chin. J. Eng.* **2018**, *40*, 127.
38. Wang, K.L.; Huang, B.C.; Liu, D.M.; Ye, D. Ordered mesoporous carbons with various pore sizes: Preparation and naphthalene adsorption performance. *J. Appl. Polym. Sci.* **2012**, *125*, 3368. [CrossRef]